DiadFit: An Open-SourcePython3 Tool for Peak fitting of Raman Data from silicate melts and CO_2 fluids

Penny E. Wieser[1] and Charlotte DeVitre[1]

Earth and Planetary Sciences, UC Berkeley

This tool is for you – the Raman and CO_2- loving community. We have posted this preprint to give you a chance to try the code. Doesn't work for your instrument or your file type? Please send me some examples, and I will tweak it so it does!

Penny_wieser@berkeley.edu, or raise an issue on GitHub - https://github.com/PennyWieser/DiadFit

DiadFit: An Open-Source Python3 Tool for Peak fitting of Raman Data from silicate melts and CO_2 fluids

Penny E. Wieser,*‡ Charlotte L. DeVitre‡

Abstract

We present a new Open-Source Python3 tool, DiadFit, for efficient processing of Raman spectroscopy data associated with silicate melts and CO_2 fluids. DiadFit can fit Fermi diads, hot bands, ^{13}C peaks, and Ne lines using various background and peak shapes. Thus, it is highly suited for workflows involving melt inclusion vapour bubbles and fluid inclusions (FI). We include generic peak fitting functions (e.g., for fitting carbonate and S-rich phases), and functions to quantify the area ratio of the silicate vs. H_2O region of spectra collected on silicate glasses to determine H_2O contents. DiadFit can convert between temperature, pressure and density using the CO_2 equation of state (EOS), allowing calculation of FI entrapment pressures (and depths in the crust) DiadFit can also calculate CO_2 density from microthermometry measurements of T_{homog}. DiadFit can propagate errors in these EOS calculations using Monte Carlo methods. Documentation and worked examples are available (`https://bit.ly/DiadFitRTD`, `https://bit.ly/DiadFitYouTube`).

1 Introduction

In recent years, Raman Spectroscopy has been increasingly used by igneous petrologists to perform non-destructive, in-situ measurements of the composition of fluids and melts (Steele-Macinnis et al. [2011], Hartley et al. [2014], Moore et al. [2015], González-García et al. [2020], Giordano et al. [2020], Schiavi et al. [2020], Morizet et al. [2013], Schiavi et al. [2018]). Since 2014, there has been a growing amount of interest in using Raman Spectroscopy to measure the density of CO_2-rich fluids in melt inclusion vapour bubbles, to obtain accurate estimates of magma storage depths (Hartley et al. [2014], Moore et al. [2015], Wieser et al. [2021] Lamadrid et al. [2017], Allison et al. [2021]). Raman spectroscopy also shows enormous potential to quantify the densities of CO_2-rich fluid inclusions (Wang et al. [2011]), allowing rapid and precise estimates of magma storage depths (Dayton et al. [2023]).

However, while there have been a large number of studies optimizing calibration and analysis protocols for CO_2 rich fluids by Raman Spectroscopy (e.g., Lamadrid et al. [2017], DeVitre et al. [2021], Bakker [2021]), there has been comparatively less focus on the software tools and peak fitting routines used to fit Raman spectral data (e.g. Yuan and Mayanovic [2017]). Many studies use proprietary instrument software for peak fitting (e.g. Moore et al. [2015]), which affects reproducibility because data is collected (and thus processed) on different Raman instruments (e.g., WITec, HORIBA, Bruker, Renishaw). One open-source option is a GUI-based peak fitting program called Fityk (Wojdyr [2010]), which was used by DeVitre et al. [2021]. However, while scripting is possible in this tool, most users fit curves by manually clicking to select peak and background positions. Other studies use OriginLab software (e.g., Hartley et al. [2014], which has an annual subscription fee of $\sim$ 200 USD per license per year), or have developed their own Matlab/Python codes for specific workflows and instruments (e.g., Wieser et al. [2021], Allison et al. [2021]). We do not believe any of the existing data processing methods have been fully optimized for the specific Raman-based workflows becoming widespread in volcanology. There are also no widely-available tools for common calculations associated with Raman data (e.g., converting measured CO_2 densities from fluid inclusions into pressure and depths using the CO_2 equation of state).

The aim of DiadFit is to provide an open-source, reproducible, easy-to-use, and efficient tool for volcanologists with a wide range of coding experience (Fig. 1). The shapes and locations of the Fermi diad and Ne lines are well defined, and spectra collected on any given Raman instrument have similar

*University of California, Berkeley

†Corresponding author: penny_wieser@berkeley.edu

‡University of California, Berkeley

features, opening up the potential for automation. As well as saving time, this will also resut in more consistent fitting between different spectra, and increase reproducibility. DiadFit is designed so that generic peak fit parameters are tweaked for a specific analytical set up. Using these tweaked parameters, hundreds of spectra can be fitted automatically within minutes, eliminating tedious (and subjective) mouse-based clicking workflows. Additionally, we encourage users to publish the Jupyter Notebook they used for peak fitting (along with the relevant metadata and spectra) in the Supporting Information, for maximum reproducibility.

For example, fitting the Neon and diad data collected over a 24 hour period during instrument calibration by DeVitre et al. [2021] took at least a day to process using Fityk, but can be processed in ~15 minutes using DiadFit on a typical laptop with 16 GB of RAM. Given the potential for Raman spectroscopy to provide rapid estimates of magma storage depths from fluid inclusions during volcanic crises (Dayton et al. [2023]), it is vital to speed up data processing as much as possible to reap the full benefits of this technique. We anticipate that users who are not familiar with Python will simply use the provided Jupyter Notebooks and narrated YouTube videos, changing simple parameters like the path to their files. More experienced coders can use the base functions in DiadFit to create highly customizable workflows to address a number of additional science questions to those targeted here (and build their own functions).

2 Installation

DiadFit package can be installed locally on Python versions >=3.7 using the command from either the command prompt (Windows) or the terminal (Mac):

```
pip install DiadFit
```

For Python beginners, we recommend using Jupyter environments (e.g., Jupyter Lab and Jupyter Notebook). In these environments, DiadFit can be installed in a code cell directly:

```
!pip install DiadFit
```

After installation, the user must load DiadFit into their script. Here we load it as `pf.` but users could choose any letters they wish:

```
import DiadFit as pf
```

Any function from DiadFit is then called by typing the chosen abbreviation, followed by a dot, followed by the function name:

```
pf.function_name()
```

Information on what the function does and the required inputs can be accessed using the help function:

```
help(pf.fit_generic_peak)
```

3 Underlying Dependencies

DiadFit uses peak-fitting functions from the Python package `lmfit` (Newville et al. [2016]), which supports iterative fitting of different peak types (e.g., Gaussian, Voigt, Pseudovoigt). The SciPy (Virtanen et al. [2020]) `find_peaks` function is used to identify approximate peaks positions and attributes (height, prominence, presence/absence of certain peaks like hotbands above a specific threshold). These estimated peak parameters can be used to subdivide spectra into groups with similar characteristics prior to fitting with `lmfit`. Grouping spectra by characteristics, as well as having good estimates of peak positions and prominences greatly increases computational efficiency during iterative fitting of multiple peaks in `lmfit` (e.g., iteratively fitting PseudoVoigt peaks for the Diad, hot-band and ^{13}C peak, along with an elevated Gaussian background superimposed on a polynomial background). Numpy (Harris et al. [2020]) is used for all basic math and regression operations, including fitting splines to spectra, and splitting spectra into particular subregions. Pandas (pandas development team [2020]) is used for importing data from spreadsheet-type datafiles (.xlsx, .csv), and to output fit parameters in a tabular format. Matplotlib (Hunter [2007]) is used for all plots produced by functions. Users will need to install all these packages first if they are not already installed (e.g., through Anaconda), and then these should be loaded at the start of each notebook:

```
import numpy as np
import pandas as pd
import matplotlib.pyplot as plt
```

4 Supported File Types

DiadFit currently supports data input from the following file types. The name given between quotes is the string that should be entered into the `filetype` argument when loading data:

1. `'headless_txt'`: txt file with no header, with wavenumber in the 1st column and intensity in the 2nd column.
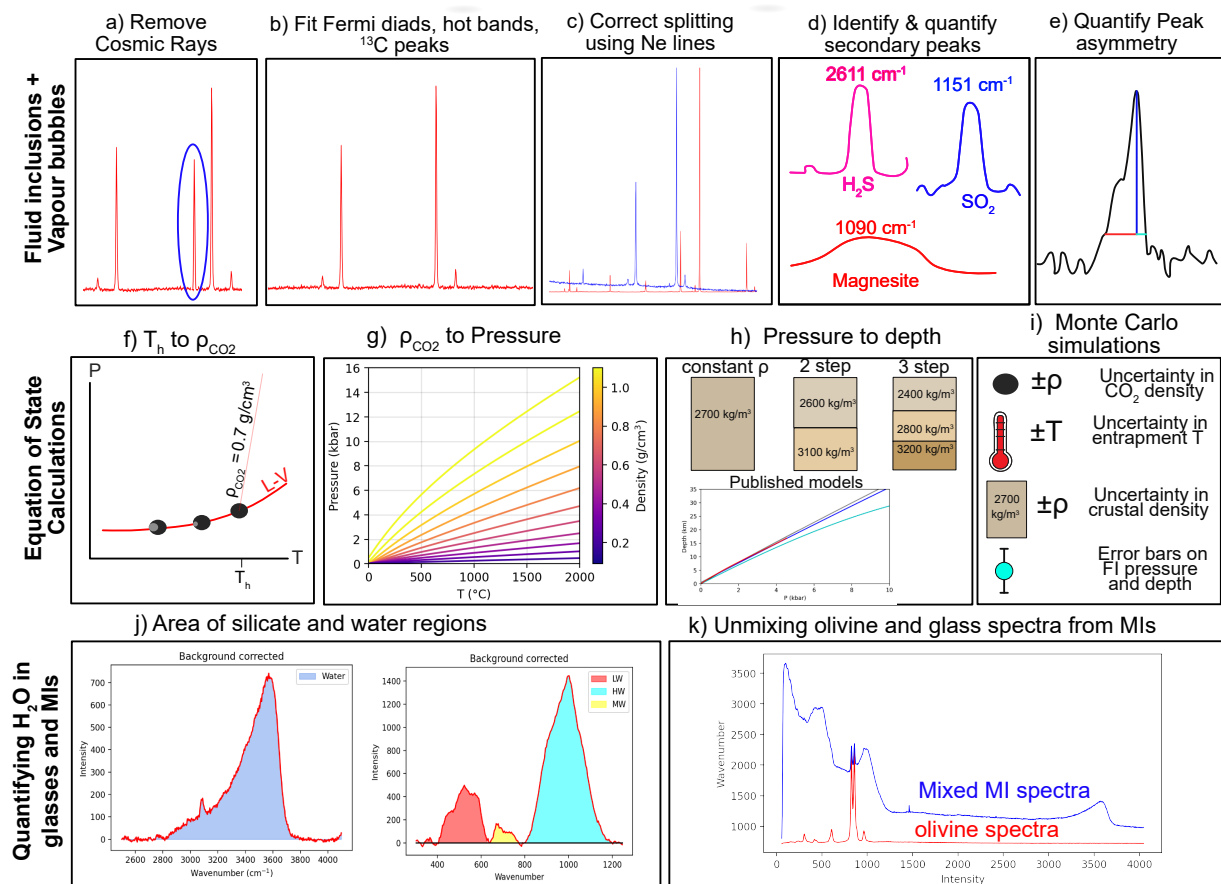
Figure 1: Schematic diagram showing the different workflows that can be performed in DiadFit.

2. `'headless_csv'`: csv file with no header, with wavenumber in the 1st column and intensity in the 2nd column.

3. `'head_csv'`: csv file with a header, with wavenumber in the 1st column and intensity in the 2nd column.

4. `'Witec_ASCII'`: Standard output from WITec Raman instruments. File starts with '//Exported ASCII-File', then has several lines of metadata, before data is listed under a [Data] heading

5. `'HORIBA_txt'`: Standard output on newer HORIBA Raman instruments. It has some metadata rows (e.g., #Acq. time), then data is listed under #Acquired

6. `'Renishaw_txt'`: Standard txt file from a Renishaw instrument, first header is #Wave, second is #Intensity

If your Raman spectrometer outputs a different filetype, please raise an issue on the DiadFit GitHub or contact the author team by email, and we will endeavor to add the required functionality.

5   Python Jargon

Functions are used to perform calculations, the user enters specific input parameters (called arguments), and the function returns various outputs. Five main datatypes are used in DiadFit:

1. A `"string"` is a piece of text. These are used to tell a function something about your data input, or specify a certain thing you want the function to do. For example, users must specify their filetype when using functions that load in spectra (e.g., `filetype='headless_txt'`, see Section 4).

2. A `numpy.array` is a column of data without a heading. DiadFit uses these to store spectral data after it has been extracted from proprietary instrument files. The wavenumber is stored in the 1st column (index 0 in Python), and the intensity in the 2nd column (index 1 in Python). The advantage of using Numpy rather than pandas is it allows for very fast computation.

3. A `pandas.Series` is a column of data with a heading.

4. A `pandas.DataFrame` is a collection of pandas.Series, and can be visualized like a single sheet in an excel workbook with labelled columns. In DiadFit, these are used to store

peak fitting parameters in columns with column headings (see Step 2, Fig. 2). Information in a given column of the dataframe (called df) can be accessed using the column heading: `df['column_heading']`.

5. `dataclasses` are used to provide default configurations to peak finding and fitting functions. These default configurations can be tweaked as much or as little as required for each specific Raman spectrometer. For example, the default parameters for fitting diad 1 are stored in the dataclass `diad1_fit_config`:

```
diad1_fit_config(model_name='PseudoVoigtModel',
fit_peaks=2, fit_gauss=False,
gauss_amp=1000, diad_sigma=0.2,
diad_sigma_min_allowance=0.2,
diad_sigma_max_allowance=5,
N_poly_bck_diad1=1,
lower_bck_diad1=(1180, 1220),
upper_bck_diad1=(1300, 1350),
diad_prom=100, HB_prom=20,
x_range_baseline=75, y_range_baseline=100,
plot_figure=True, dpi=200,
x_range_residual=20)
```

Briefly, `model_name='PseudoVoigtModel'` specifies that the diad and hotband peaks should be fitted with a PseudoVoigt function, which is a weighted sum of a Gaussian and Lorentzian distribution that share values for amplitude, center, and full width half maximum. A Voigt distribution function can be used instead simply by stating:

```
pf.diad1_fit_config(model='VoigtModel')
```

Any number of these parameters can be tweaked. For example, if the user only wants 1 peak (e.g., for weak spectra), wants to fit a third degree polynomial to the background, and wants saved figures showing spectra fits to have a dpi of 300:

```
diad1_fit_config(model='VoigtModel',
fit_peaks=1, N_poly_bck_diad1=3, dpi=300)
```

The idea is once these dataclasses are tweaked for a given instrument/set of samples, they can be used to automatically loop through large numbers of files. Detailed information on any of these arguments can be found in the documentation.

6   Worked Examples

We have produced a number of Jupyter Notebooks showing detailed examples of how to perform different workflows. These notebooks are available on GitHub and the ReadTheDocs page. For example, we include notebooks showing how to:

1. Fit peaks resulting from CO_2 fluids (diads, HBs, ^{13}C peaks), calculate diad splittings, and correct these using Ne acquisitions. In this example, we use data collected from a high pressure optical cell during Raman densimeter calibration (see DeVitre et al. [2021]).

2. Fit CO_2 peaks, apply a Ne correction model to diad splittings, and quantify the heights and areas of carbonate and SO_2 peaks in spectra collected from fluid inclusions hosted in olivine crystals.

3. Fit CO_2 diads and apply a Ne correction model from spectra collected from melt inclusions vapour bubbles using a HORIBA Raman instrument (data from Wieser et al. [2021]).

4. Quantify peak asymmetry in spectra collected at room temperature with densities between $\sim$ 0.2–0.7 g/cm^3 using the approach of DeVitre et al. [2023].

5. Quantify H_2O contents in silicate glasses using an approach adapted from Di Genova et al. [2017] and Schiavi et al. [2018].

6. Quantify the ratio of H_2O to silicate glass peaks on Raman acquisitions taken on unexposed olivine-hosted melt inclusions. This can also be used to quantify H_2O in exposed glasses (following Di Genova et al. [2017]).

7. Calculate various parameters using the CO_2 equation of state, including converting homogenization temperatures from microthermometry into CO_2 densities, converting CO_2 densities from Raman or microthermometry into pressures, and then converting these pressures to depths using different crustal density profiles.

8. Notebooks showing how to propagate uncertainty in microthermometry and Raman-based fluid inclusion barometry into pressure and depth distributions.

7 FITTING NE LINES

During any given analytical session, there may be some stretching or contraction of the Raman spectra; these changes are often referred to as 'non-linearity of the Raman shift axis'. For brevity and to draw parallels with various mass spectrometry techniques, we term this 'instrument drift'. We find that these changes often correlate very well with temperature changes in the laboratory. Commonly, instrument drift within the spectral region containing the Fermi diad is assessed by repeatedly measuring the emission spectrum of Neon (Ne) produced by a

lamp every $\sim$ 5-10 minutes. As well as correcting drift during a given session, Ne can also be used to apply a correction factor between sessions, allowing continued use of a Raman densimeter months to years after it was calibrated.

The Ne emission spectrum has a number of distinctive "lines", several of which lie close to the position of the CO_2 Fermi diad. The wavelength of the different Ne lines in air (λ_1) are converted into Raman shifts (Δ_ν) in cm^{-1} using the excitation wavelength of the laser (e.g., λ_0=532.05 nm; Lin et al. [2007]):

$$\Delta_\nu = \frac{10^7}{\lambda_0(nm)} - \frac{10^7}{\lambda_1(\text{nm})} \qquad (1)$$

Traditionally, a given diad acquisition has been corrected for instrument drift and non-linearity by comparing the measured distance between two selected Ne lines ($\Delta_{Ne}^{\text{Measured}}$) and the theoretical distance between those lines using Equation 1 ($\Delta_{Ne}^{\text{Theoretical}}$):

$$\text{Correction Factor} = \frac{\Delta_{Ne}^{Theoretical}}{\Delta_{Ne}^{Measured}} \qquad (2)$$

This correction factor is then used to correct the measure diad splitting:

$$\Delta_{CO_2}^{Corrected} = \text{Correction Factor} \times \Delta_{CO_2}^{Measured} \qquad (3)$$

This approach has been termed the 'line segment' technique by Bakker [2021], and a typical workflow of how this method is performed in DiadFit is summarized in Fig. 2. Step 1 identifies all the files which contain Ne lines. This can either be achieved by specifying the path to a folder containing just Ne line acquisitions, or by specifying a a unique 'string' that only Ne lines have in their file name (if all spectra from one day are stored in a single folder). In the following code snippet, we obtain all the '.txt' files in the folder 'spectra_path' containing the characters 'Ne'. If some of your other acquisitions also include this string, you can exclude other strings to help isolate the right files (here we do not want to include files with the name 'FG' or 'Ol'):

```
Ne_files=pf.get_Ne_files(path=spectra_path,
file_ext='txt', ID_str='Ne',
exclude_str=['FG', 'Ol'])
```

Step 2 calculates the theoretical wavenumber of each Ne line using the specific wavelength of your Raman system. You can specify a threshold intensity, and only get lines stronger than that (here, we set the threshold at 2000). This returns a dataframe, with the Raman shift (wavenumber) expected for each Ne line position for your specific wavelength (See Fig. 2 Step 2):
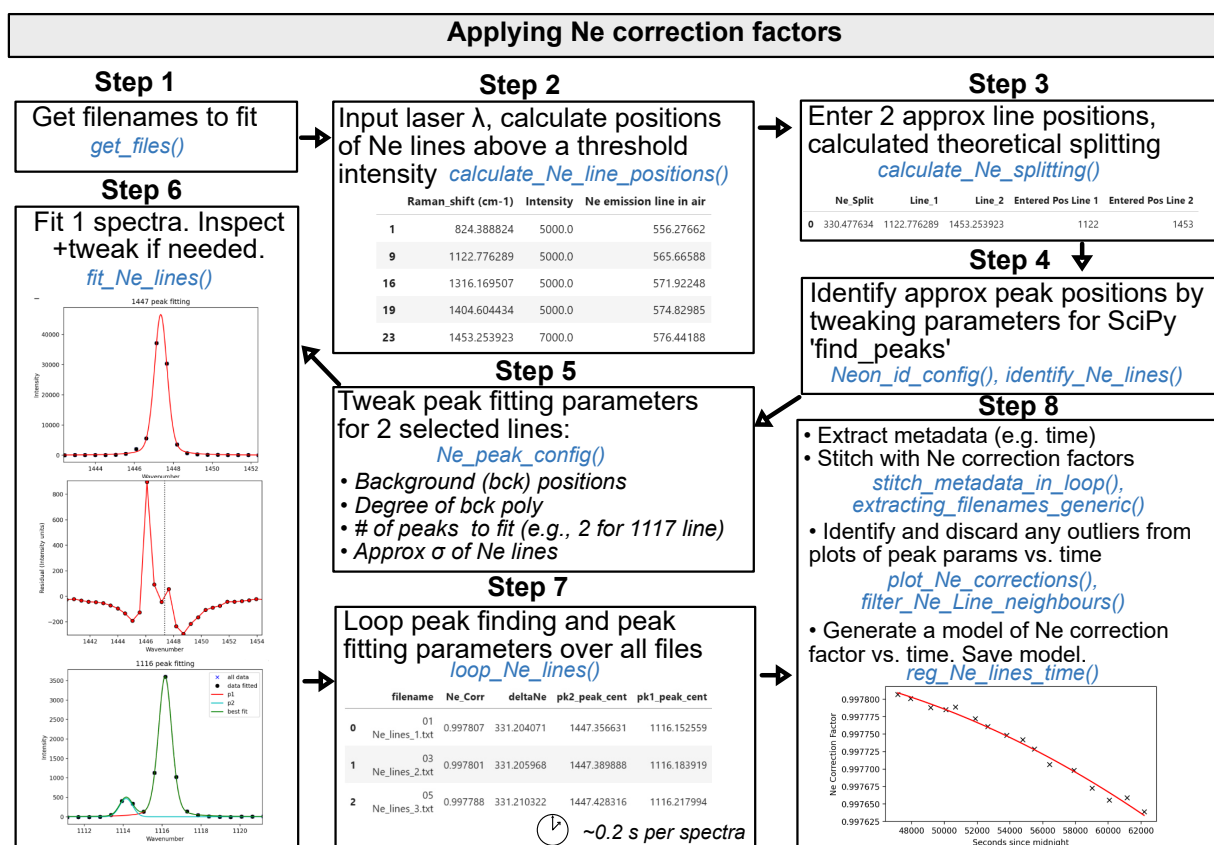
Applying Ne correction factors

Step 1

Get filenames to fit
get_files()

Step 6

Fit 1 spectra. Inspect +tweak if needed.
fit_Ne_lines()

Step 2

Input laser λ, calculate positions of Ne lines above a threshold intensity *calculate_Ne_line_positions()*

	Raman_shift (cm-1)	Intensity	Ne emission line in air
1	824.388824	5000.0	556.27662
9	1122.776289	5000.0	565.66588
16	1316.169507	5000.0	571.92248
19	1404.604434	5000.0	574.82985
23	1453.253923	7000.0	576.44188

Step 5

Tweak peak fitting parameters for 2 selected lines:
Ne_peak_config()
• *Background (bck) positions*
• *Degree of bck poly*
• *# of peaks to fit (e.g., 2 for 1117 line)*
• *Approx σ of Ne lines*

Step 7

Loop peak finding and peak fitting parameters over all files
loop_Ne_lines()

	filename	Ne_Corr	deltaNe	pk2_peak_cent	pk1_peak_cent
0	01 Ne_lines_1.txt	0.997807	331.204071	1447.356631	1116.152559
1	03 Ne_lines_2.txt	0.997801	331.205968	1447.389888	1116.183919
2	05 Ne_lines_3.txt	0.997788	331.210322	1447.428316	1116.217994

🕐 *~0.2 s per spectra*

Step 3

Enter 2 approx line positions, calculated theoretical splitting
calculate_Ne_splitting()

	Ne_Split	Line_1	Line_2	Entered Pos Line 1	Entered Pos Line 2
0	330.477634	1122.776289	1453.253923	1122	1453

Step 4

Identify approx peak positions by tweaking parameters for SciPy 'find_peaks'
Neon_id_config(), identify_Ne_lines()

Step 8

• Extract metadata (e.g. time)
• Stitch with Ne correction factors
stitch_metadata_in_loop(), extracting_filenames_generic()
• Identify and discard any outliers from plots of peak params vs. time
plot_Ne_corrections(), filter_Ne_Line_neighbours()
• Generate a model of Ne correction factor vs. time. Save model.
reg_Ne_lines_time()

Figure 2: Schematic showing how DiadFit can be used to fit Ne lines, and build a model of correction factor vs. time.

```
df_Ne=pf.calculate_Ne_line_positions(
wavelength=531.885, cut_off_intensity=2000)
```

In Step 3, two Ne lines are selected (1122 and 1453 in this example), and the theoretical splitting is calculated between the closest lines to those specified wavenumbers. In Step 4, one representative file is selected, and used to tweak peak identification parameters, which are then fed into the Scipy `find_peaks` function to identify the approximate position of each Ne line (and its intensity). Obtaining approximate peak positions and intensities greatly improves the computational efficiency of the fitting process. Default peak identification parameters are stored in the data class `Neon_id_config`, such as the height, prominence, width and threshold to use when identifying peaks using SciPy `find_peaks`. The prominence, defined as the vertical distance above the neighbouring background, is the most important parameter to tweak between different instruments (some instruments have peaks hundreds to thousands of counts above background, others have hundreds of thousands to millions of counts above background). The function `identify_Ne_lines` uses this tweaked configuration file, and identifies the largest peak within ± 10 datapoints of the Ne line of interest (e.g. for a spectra resolution of 0.4 cm^{-1} and for line 1122, the spectra between 1118-1126 cm^{-1} would be searched).

After approximate peak positions for each file have been identified in Step 4, peak fitting parameters need to be tweaked in Step 5. The peak fitting function fits a polynomial background to two regions either side of the Ne line, discarding points within this region which are outside of a certain number of standard deviations of the median background position (default 3σ, can be tweaked in `Ne_peak_config`). This background is then subtracted. For most Ne lines, a single PseudoVoigt/Voigt curve can be fitted to background-subtracted data (See ~1447 cm^{-1} peak in Step 6, Fig. 2). For the line at ~1116 cm^{-1}, two peaks need to be fitted iteratively because of the prominent shoulder to the left of this line (red and cyan curves, combined into the green curve, Fig. 2). Default values specifying how to fit these peaks are stored in a dataclass `Ne_peak_config`, and generally only need tweaking once for each instrument and each selected Ne line. The most important parameters are the positions of the background. These are expressed in terms of distance from the peak center identified above. For example, specifying `lower_bck_pk1=(-40, -25)` positions a background window 40-25 wavenumbers to the left of the peak center. Other important parameters include the degree of polynomial to fit between background points `N_poly_pk1_baseline=2`, and the

approximate sigma of the PseudoVoigt/Voigt curve (`pk1_sigma=0.6`, `pk2_sigma=0.7`). In Step 6, these tweaked peak fit parameters are used to fit one spectra file with the function `fit_Ne_lines`. This function returns the peak positions and other fit parameters, as well as graphs showing the overall best fit, the residual of the fit, and the background positions. In addition to plots for visual inspection of residuals, the function also calculates a measure of the residual for each peak:

$$Residual = \frac{\sum \sqrt{(y_{meas} - y_{fitted})^2}}{N_{points}} \qquad (4)$$

where y_{meas} is the y-coordinate of the background-subtracted data, y_{fitted} is the y coordinate of the best composite model fit, and N_{points} is the number of discrete points along the x axis used in the fit.

After inspecting these graphs for one Neon acquisition and tweaking any fit parameters as necessary (e.g., background positions, plotting parameters), the `Ne_peak_config` file is updated with the sigma values obtained from this example file (rather than the users guess). The tweaked find peaks and peak fit parameters can then be used to loop through all Ne spectra (Step 7). On a regular laptop (e.g., 16 GB RAM, Intel i7), it takes approximately 0.2 s to fit each Ne file. There is also an option for the function to save a figure showing the fit for each file in a subfolder it creates within the spectra path. This increases the run time to 1.2 s for each file, but allows users to check the fits (or publish fits as part of a data repository accompanying a paper). After all files are looped through, DiadFit returns a pandas dataframe with the filename, and all the peak fit parameters (including the all important Ne correction factor).

In most published studies, Fermi diad acquisitions have been corrected using the average correction factor of the Ne line acquired before and after that specific sample (or on certain instruments, Ne is collected concurrently with diads). However, the relatively narrow shape of the Ne peaks means that there is a degree of random noise associated with peak fitting. Thus, we suggest it may be better to perform a regression of the correction factor as a function of time, which can then be applied to samples. On many instruments (e.g., WITec, some HORIBAs), the spectral file doesn't include a time stamp. Sometimes (e.g., WITec), the timestamp is stored in the metadata file, meaning that data and metadata files must be stitched together to obtain the time for each Ne correction factor (see documentation for examples). Alternatively, if the instrument outputs each spectra file during the acquisition, DiadFit contains functions to extract the time based on the read or edit time stamp on the file. Once a DataFrame is obtained that contains

both the Ne correction factor and the time (Step 8), it is useful to inspect changes in Neon correction factors and peak positions with time using built-in visualization functions (e.g., `plot_Ne_corrections`). This allows outliers to be discarded that differ substantially from adjacent acquisitions using the function `filter_Ne_lines_neighbours`. Finally, a polynomial or spline model is used to parameterize the change in Ne correction factor as a function of time (expressed as seconds after midnight, Step 8, Fig. 2). This correction model can then be saved, and loaded into a notebook used for Diad Fitting to correct data from the same session. These smoothed correction factors can then be applied to the measured diad splitting.

7.1 A more complex Ne fitting routine

Bakker [2021] criticized the 'line segment' technique, because it assumes that the correction factor at any given point between two lines is the the same. Any non-linearity in the spectrometer invalidates this assumption (Bakker [2021]). It has also been noted that the choice of different Ne lines bracketing the Fermi diad greatly influences the correction factor (and even the direction of drift within a given analytical session, (Wieser et al. [2021]). Bakker [2021] suggest that a model should be developed for how the position of measured Ne lines deviates from the true theoretical position as a function of wavenumber, allowing a correction factor to be applied to each diad position (these corrected diad positions should then be used to calculate splitting). They term this the 'bracketing' technique. Fig. 3a shows the position of Ne lines relative to the Fermi diad from a fluid inclusion collected using a green laser with λ=532.046 nm. Fig. 3b shows the deviation of each Ne line from the theoretical position (theoretical/measured position) for 6 different Ne lines over a 24 hour period. For each Ne acquisition, we fit a polynomial through the correction factor for 6 Ne lines to describe the shift as a function of the wavenumber for each discrete acquisition.

These polynomial fits demonstrate that the correction factor is highly non linear across the spectral window of interest. The 'line segment' technique can be visualized by drawing a straight line between any two points on a polynomial curve (Fig. 3c). If the gradient of this linear segment is the same as the gradient of a line drawn between the locations where the diad peaks intercept the polynomial, the line segment technique provides a reasonable approximation of the correction factor. However, it is clear that applying the line segment technique to the 1220-1567 lines (red dashed segment) would result in a Ne correction factor that is far smaller than that determined using the bracketing technique (ΔCF_{brack}=0.9977

vs. $\Delta CF_{segment}$=0.9991), resulting in a higher apparent diad splitting ($\Delta CO2_{brack}$=103.450 vs. $\Delta CO2_{segment}$=103.648 cm^{-1}). In contrast, the line segment method applied to the 1220-1400 lines results in a very similar correction factor to the bracketing technique (ΔCF_{brack}=0.9977 vs. $\Delta CF_{segment}$=0.9976). However, the disadvantage of this combination of lines is that the 1220 line is relatively small, resulting in larger fitting errors, meaning that correction factors show substantially more variability in a given run than using the 1117–1447 pair.

While the absolute correction factor clearly varies as a function of the choice of Ne line correction method, in terms of quantifying CO$_2$ diads, it is more important to determine how these Ne correction factors change within and between runs. If the offset between the bracketing and line segment techniques is constant, then as long as the relationship between CO$_2$ density and diad splitting is calibrated using the same Ne correction technique that is used during instrument measurement, it may not matter. The tedium of fitting Ne lines in existing tools means that very few studies have investigated the relative drift of different Neon correction routines. DiadFit allows users to easily fit all relevant lines, so non-linearities specific to each individual Raman instrument can be investigated to develop the best Ne correction strategy.

8 FITTING THE CO$_2$ FERMI DIAD

The Raman spectrum of CO$_2$ consists of two relatively strong, well-defined peaks collectively called the Fermi Diad. These peaks result from the interaction of a symmetrical stretching mode and an active bending mode in the CO$_2$ molecule by a process known as Fermi resonance (Lamadrid et al. [2017], Rosso and Bodnar [1995], Fermi [1931]). One of the peaks has a wavenumber of ~1280–1290 cm^{-1} (refered to as diad 1), and the second peak has a wavenumber of ~1386–1390 cm^{-1} (diad 2, Fig. 3a). It is well accepted that the distance between the diad 1 and diad 2 (commonly referred to as splitting, diad splitting, Fermi Diad separation, or Δ) correlates with the density of the CO$_2$ fluid. This is because with increasing CO$_2$ density, diad 1 moves to lower wavenumbers (shift of 6 cm^{-1} from 0 to 0.8 g/cm^3), while the position of diad 2 only varies by ~1–2 cm^{-1}. The exact relationship between diad splitting and CO$_2$ density, commonly called a 'densimeter', has been shown to vary as a function of instrument hardware and acquisition conditions, so must be calibrated for each analytical set up (DeVitre et al. [2021], Lamadrid et al. [2017]).

The Fermi diad is flanked by low intensity hot bands (HBs), which arise from molecules populating the first excited vibron due to their thermal en-
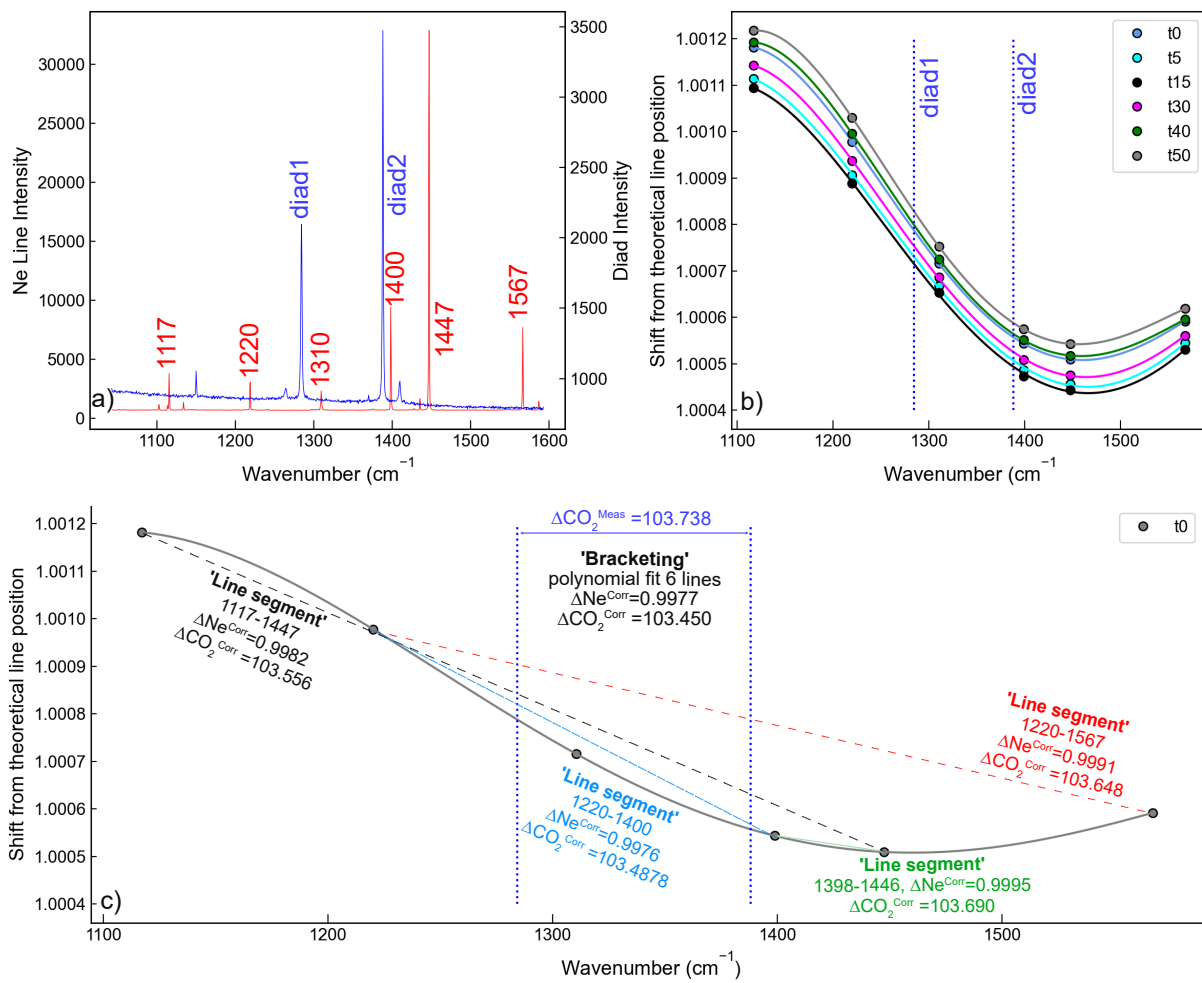
Figure 3: Schematic showing how DiadFit can be used to fit Ne lines, and build a model of correction factor vs. time.

ergy at room temperature, which are also perturbed by a Fermi resonance effect. The peak height of the HBs relative to the diads increases with increasing temperature (Rosso and Bodnar [1995]), and in general, hotbands become more pronounced in spectra collected on denser CO_2 fluids. Diad 2 also has a flanking ^{13}C peak to its left which becomes more visible as the CO_2 density increases and with increasing proportions of ^{13}C relative to ^{12}C (Wang and Lu [2022]).

In the literature, density estimates from CO_2-rich fluids such as melt inclusion vapour bubbles or fluid inclusions have been obtained by fitting the position of the Fermi diad using various background models combined with Voigt, Pseudovoigt, Gaussian or Lorentzian peaks. These peak fitting routines greatly increases the precision at which the diad splitting can be determined relative to the spectral resolution of the instrument (distance between datapoints). While Raman instruments typically acquire an intensity reading every 0.1–1.5 cm^{-1}, the error of the peak position on a fitted peak can be 10–30× smaller if an appropriate peak profile is fitted (e.g., voigt/pseudovoigt for diads, Yuan and Mayanovic [2017], Fukura et al. [2006]; Lin et al. [2007]). After the peaks are fit, the splitting is calculated and corrected for instrument drift, and then an instrument-specific densimeter should be used to convert splitting into CO_2 density (Lamadrid et al. [2017], DeVitre et al. [2021]).

Step 1 is to find all the spectral files you wish to fit (Fig. 5). Unlike Ne lines, which all have similar intensities, diads can vary greatly in appearance. For example, spectra collected on CO_2 fluids with low densities, at greater depth in the sample, or using low laser power, tend to have a weak to non existent hot band. Stronger spectra have prominent hot bands and ^{13}C peaks, which overlap with the tail of the diad peak. The strongest spectra have a ^{13}C peak, and the entire region around the diads and hotbands is elevated above the near-linear background around the diads (Fig. 4). Thus, we suggest users subdivide their spectra into 'weak', 'medium' and 'strong' diads, and tweak fitting parameters to each group. This allows automated spectral fitting within each group.

DiadFit contains a number of functions to subdivide spectra into these groups. In Step 2 (Fig. 5), a single file is selected, and the `identify_diad_peaks` function uses SciPy `find_peaks` to obtain approximate peak positions and prominence of the diad, hotbands and ^{13}C peaks for each spectra, as well as various parameters quantifying the signal to noise ratio, and the elevation of the diad-HB region above background. As for Ne lines, the Scipy `find_peaks` parameters will need tweaking based on instrument hardware and acquisition parameters to ensure the function

finds all peaks which are visible, and doesn't identify noise as peaks (identified peaks are marked with yellow stars in Step 2). After tweaking these SciPy parameters, all spectra files are looped over to determine the approximate peak parameters for each spectra, and these are saved in a dataframe. In Step 4, these peak parameters are used alongside a filter to remove any cosmic rays present in the spectra. The filtering process calculates the intensity factor F based on the intensity (I) of any given spectral datapoint relative to the intensities of the datapoints to the left and right:

$$F_{i-1} = \frac{I_i - I_{i-1}}{I_{i-1}} \tag{5}$$

$$F_{i+1} = \frac{I_i - I_{i+1}}{I_{i+1}} \tag{6}$$

These two factors are then multiplied together:

$$M_i = F_{i-1} * F_{i+1} \tag{7}$$

If the spectra has a lower intensity to the left of datapoint i, F_{i-1} will be >1. If the spectra also has lower intensity on the right hand side of point i, F_{i+1} will be >1, so M_i will be >>1. High values of M_i for individual pixels are indicative of short, sharp peaks (i.e. most cosmic rays). A datapoint is considered a cosmic ray if M_i exceeds a user determined value (`dynfact`). The highest pixel of Diads, HB and ^{13}C peaks can also have high M_i values, so any points with an x coordinate equal to an identified peak position (± the spectral resolution) are ignored. Users can also enter a custom range, within which no cosmic rays are removed (e.g. the area around the narrow SO_2 peak). If a cosmic ray is identified, the filter is run again, in case the cosmic ray was wider than a single pixel. The pixels identified as cosmic rays are then removed from the spectrum and a new file is saved with the same filename with the addition of the suffix `_CRR_DiadFit`. After removal of cosmic rays, the `identify_diad_peaks` function is used again to obtain approximate peak parameters without inference from cosmic rays.

In Step 5, the approximate peak parameters from `identify_diad_peaks` are used to classify spectra into groups. A full description of the different parameters used for classification is provided on the ReadTheDocs page, and the most useful parameters will depend greatly on your Raman instrument and samples. In general, spectra should be classified as 'Weak' when none of the peaks are strong enough to interfere with each other (e.g., Fig. 4c). In a set of acquisitions where lots of spectra have no hot band, it would make sense to have the weak group be spectra with only a diad, and no HB. These are best fitted with a single peak (`fit_peaks=1`). If there was then a second group of slightly stronger spectra with a relatively prominent hot band, these

could be classified as 'Medium', with 2 peaks fitted around diad 1, and 3 peaks around diad 2. Fitting more peaks peaks helps improve the overall residual because the tails of the diad and hotband peak overlap slightly for higher CO_2 densities, so should be fitted iteratively (Fig. 4f). Spectra with very strong hot bands, clear ^{13}C peaks, and greatly elevated troughs between diads and HBs should be placed into the 'Strong' category. These spectra will need to be fitted with two/three peaks, and an additional Gaussian background to recreate the elevation of the spectra in the diad region (`fit_gauss=True`).

In the gas-cell calibration data of DeVitre et al. [2021], all spectra had a visible hotband. Thus, we use the 'Weak' category for spectra with no ^{13}C peak, and no overlap of the tails of HB2 and Diad2 (Fig. 4c). The remaining spectra could be split in two ways. One option is to classify them all as strong (requiring 3 peaks, and a Gaussian background). If a Gaussian background isn't really required (e.g., Fig. 4f), the code will converge on a Gaussian with a very small amplitude, so the only real advantage of putting those not really needing Gaussian backgrounds into a 'Medium' Category is that the iterative fitting routine will be a bit faster (so it is worth the extra category if you have a lot of spectra).

After tweaking the fit parameters to use for each group, one file from each group should be fitted, and the fit parameters tweaked if necessary (Step 6, Fig. 5). After this, the files in each group are looped through and fit (taking 1-5 s per spectra on a 16 GB laptop). A figure of each fit is produced, and should be visually inspected (Step 8). In Step 9, fit parameters for the different groups are merged together, and combined with any metadata (e.g. the time stamp, allowing the Ne correction model to be applied). In Step 10, splittings corrected for instrument drift should be converged into CO_2 densities using a instrument-specific densimeter.
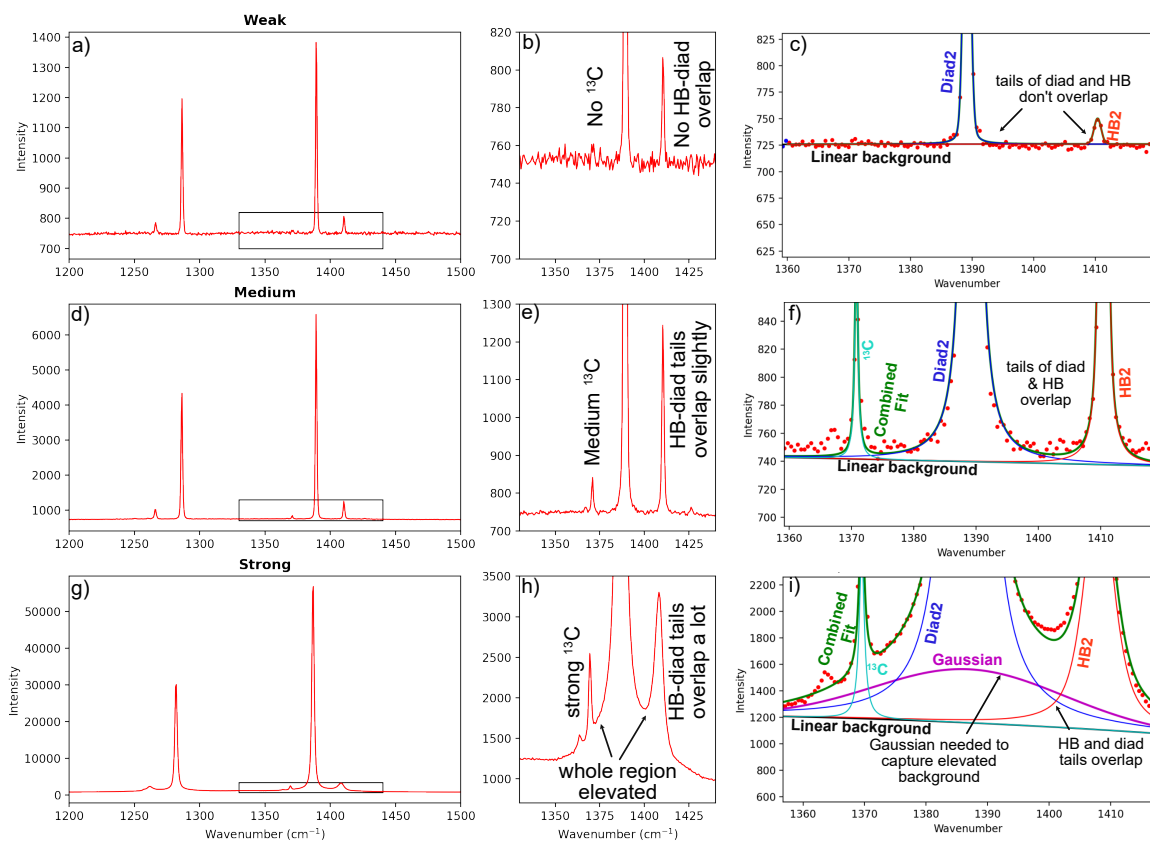
Figure 4: Example classification of spectra from DeVitre et al. [2021] with different characteristics into groups. The weakest spectra (a-c) have no ^{13}C peak, and a small HB, which does not overlap with the diad (c). These could be fitted with 1 or 2 peaks (because the fitting of the HB doesn't influence the fitting of the diad). Slightly stronger spectra (d-f) have a ^{13}C peak, and the tails of the ^{13}C, diad and HB peak all overlap (f). The overlapping tails of these peaks means that 3 peaks need to be fitted. In the strongest spectra (g-i), the troughs between ^{13}C and the diad and the diad and the HB are greatly elevated above the background. This requires fitting a Gaussian background in addition to the polynomial background, and 3 other peaks.

Fitting Fermi Diads

Step 1
Get filenames to fit
get_files()

Step 2
Identify approx peak positions by tweaking SciPy 'find_peaks'
diad_id_config(), identify_diad_peaks()

Step 3
Loop over all files to find approx peak positions, heights, etc.
loop_approx_diad_fits()

	filename	Diad2_pos	Diad2_prom	Diad1_pos	Diad1_prom	HB2_pos	HB2_prom
0	Cap19-05X1.txt	1389.651198	302.749985	1286.444974	216.699982	1410.359982	19.300018
1	Cap19-05X2.txt	1389.119077	283.750046	1286.444974	201.499970	1410.889851	25.100006
2	Cap19-06X1.txt	1389.119077	1506.349914	1285.901945	848.500000	1410.359982	94.700012
3	Cap19-06X2.txt	1389.119077	1897.249954	1286.444974	1056.399994	1410.359982	153.699982
4	Cap19-07X1.txt	1389.651198	74.449997	1286.444974	42.299988	NaN	NaN

Step 7
Fit 1 spectra. Inspect +tweak if needed.
fit_diad_1_w_bck()
fit_diad_2_w_bck()

Overall fit for Diad1

Individual fit components

Inspect residuals

Step 6
For each group, set fit parameters
diad1_fit_config()
diad2_fig_config()
• *Background (bck) positions*
• *Degree of bck poly*
• *# of peaks to fit(Diad, HB, C13)*
• *Addition of gaussian bck?*
• *Approx σ of diad*

Step 4
Check for cosmic rays, remove if present
cosmicray_filter(), filter_singleray(), filter_raysinloop()

Step 5
Sort files into Weak, Medium and Strong (based on approx fit parameters)
plot_peak_params(), filter_splitting_prominence(), identify_diad_groups(), plot_diad_groups()

Step 8
• For each group, fit all files using these parameters
• Save fit parameters
Repeat for each group
1-5 s per spectra

Fit secondary peaks if relevant (see Fig. 6)

Step 9
• Merge fits for different groups together
• Extract metadata (e.g. time), stitch with fits
• Load Ne correction model, apply to splittings
stitch_metadata_in_loop(),
extracting_filenames_generic()

Step 10
• Convert splitting to density using instrument specific densimeter

Figure 5: Schematic of workflow used to efficiently fit diad peaks with very different spectral characteristics.

8.1 Fitting peaks to secondary phases

Raman spectra collected from fluid inclusions and melt inclusion vapour bubbles commonly contain peaks arising from other gaseous species (e.g., SO_2, N_2) or solid phases on the inclusion wall (e.g., carbonates, sulfates, Schiavi et al. [2020], Frezzotti et al. [2012]). It can be helpful to identify which spectra contain such phases, and quantify parameters about these peaks (e.g., peak heights, ratio of carbonate peak area to diad peak area, Burke [2001]). To identify and quantify secondary peaks in diad fit, the first step is to obtain all the spectra you wish to fit (Fig. 6). Step 2 uses the function `plot_secondary_peaks` to plot the spectra in a specific wavenumber range from all selected files. Intensities are normalized based on the range of intensities in the selected wavenumber window, allowing multiple spectra to be stacked and inspected. It is clear from this visualization strategy that files # 42 and #33 in Step 2 of Fig. 6 have prominent carbonate peaks. For any given set of spectra, you can inspect as many regions as you want. For example, the second panel in Step 2 is centered around the SO_2 peak at ~1151 cm^{-1}. SO_2 peaks identified in Fig. 6 are shown in yellow.

In contrast to just plotting spectra to visually identify secondary phases (`just_plot=True`), the function `plot_secondary_peaks` also has two methods to identify peak positions. As well as entering a range of x coordinates to plot (`xlim_plot`) users must select a range of x coordinates to look for peaks between (e.g., `xlim_peaks=[1060, 1110]`). Then, if `find_peaks_filter=True`, the function takes the highest peak identified with scipy `find_peaks` (the user can tweak the values for prominence, height, threshold, distance and width in the function). Alternatively, `sigma_filter=True`, the code finds the highest y coordinate in the range defined by `xlim_peaks`. This is classified as a peak if it is more than N σ above the median y coordinate in that range (N is specified as `sigma=3`). For different sets of spectra, one filters may show superior performance. If either of these two filters are selected, identified peaks will be marked on the returned figure with a yellow star. The function also returns a dataframe of peak parameters (position, height, prominence, and the filename). If no peaks are found, the first three columns are filled with NaNs. These values are then used to identify spectra which contain a peak you wish to try to fit.

Peak fitting parameters for the secondary phase of interest should be tweaked in Step 3 by selecting a representative spectra. Users have the option to fit Gaussian, PseudoVoigt or Voigt peaks (through the `model_name` parameter). These tweaked parameters can then be applied to loop through all files where peaks were found in Step 2. These fitted peak parameters are then saved to an Excel spreadsheet.

More than 1 secondary phase can be identified in a given notebook. In Step 5, all identified secondary peaks are merged together with diad peak fitting parameters (see Fig. 5).
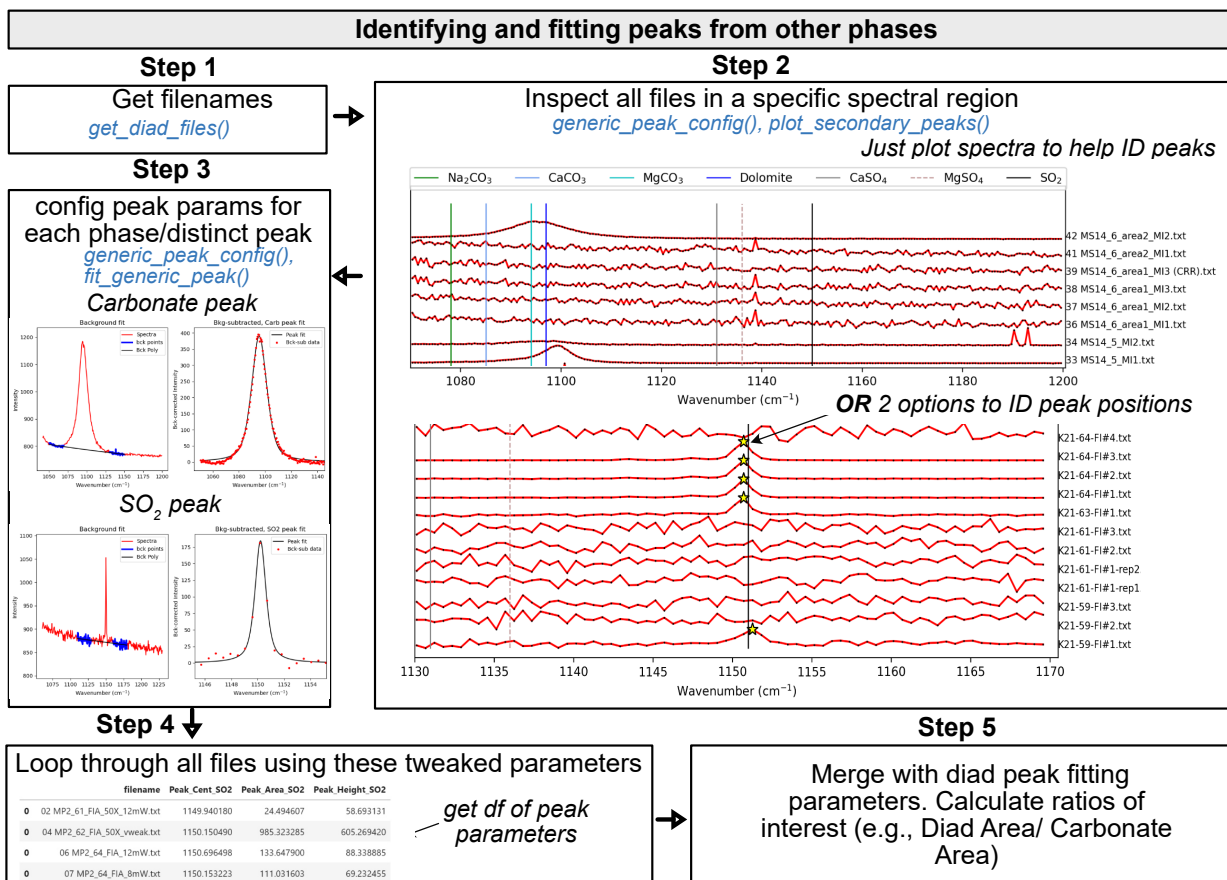
Figure 6: Schematic of workflow used to fit secondary peaks (e.g., carbonate, SO_2). Multiple secondary peaks can be fitted, and all outputs can be merged in Step 5.

9   Calculations involving the CO_2 equation of state

An equation of state (EOS) describes the relationship between physical properties of a system such as pressure, temperature and density. At the moment, DiadFit only supports calculations using the EOS for pure CO_2; in systems in equilibrium with mixed fluids (e.g. H_2O in arc magmas), the additional complexities of mixed fluids must be accounted for (see Hansteen and Klugel [2008]).

DiadFit can perform calculations using the CO_2 EOS of Sterner and Pitzer [1994] (hereafter SP94) and Span and Wagner [1996] (hereafter SW96). We implement the SP94 EOS of directly, and perform calculations using the SW96 EOS through the Python package CoolProp. This means that if users want to use SW96, they must install CoolProp on their computer (e.g., using `pip install CoolProp` or `conda install conda-forge::coolprop`). Remember, don't mix pip and conda installations if you can avoid it! Calculations using this EOS should cite both DiadFit and CoolProp. There are three core functions used to perform EOS calculations in DiadFit:

1. `calculate_rho_for_P_T` calculates CO_2 density of P and T are constrained

2. `calculate_P_for_rho_T` calculates P if CO_2 density and T are constrained

3. `calculate_T_for_rho_P` calculates T if P and CO_2 density are constrained

9.0.1   Calculating CO_2 density from pressure and temperatures

The function `calculate_P_for_rho_T` can be used to calculate CO_2 density for a specified Pressure (P) and Temperature (T). This calculation is very useful when processing data from Raman calibration apparatus, where T is measured by a thermistor, and P is measured with a pressure transducer (DeVitre et al. [2021]). An entire spreadsheet of pressures could be imported:

```
df=pd.read_excel('Cali_Data.xlsx')
dens_SW96=pf.calculate_rho_for_P_T(
P_kbar=df['P_kbar'], T_K=df['T_K'], EOS='SW96')
```

9.1   Calculating pressures from CO_2 densities and temperatures

The function `calculate_P_for_rho_T` can be used to calculate pressure for a specified CO_2 density (rho) and temperature (T). This calculation is commonly used to calculate the entrapment pressure of a fluid inclusion (assuming that the volume and

mass of the inclusion is fixed from the point of entrapment to the point at which it is measured in the lab, Roedder [2018]). For example, to convert a CO_2 density of 0.5 g/cm^3 into a pressure at a temperature of 1200 K using the Span and Wagner [1996] EOS (SW96):

```
P_SW96=pf.calculate_P_for_rho_T(
CO2_dens_gcm3=0.5, T_K=1200, EOS='SW96')
```

	P_kbar	P_MPa	T_K	CO2_dens_gcm3
0	1.721807	172.180688	1200	0.5

The Sterner and Pitzer [1994] EOS (SP94) can be used instead simply by changing the EOS argument:

```
P_SP94=pf.calculate_P_for_rho_T(
density_gcm3=0.5, T_K=1200, EOS='SW94')
```

This function can also be applied to a pandas dataframe with as many rows as the user wants. For example, we could load an entire spreadsheet with columns for CO_2 densities and an estimate of entrapment temperatures in °C (as well as an optional column with the sample name):

```
df=pd.read_excel('FI_densities.xlsx')
P_SW96=pf.calculate_P_for_rho_T(
T_K=df['Temp in C']+273.15,
CO2_dens_gcm3=df['Density_g_cm3'],
EOS='SW96', Sample_ID=df['Sample'])
```

This returns a pandas dataframe with calculations done for each input row.

	P_kbar	P_MPa	T_K	CO2_dens_gcm3	Sample_ID
0	0.276826	27.682633	1373.15	0.1	FI1
1	1.559737	155.973743	1473.15	0.4	FI2
2	3.789037	378.903651	1423.15	0.7	FI3
3	10.626112	1062.611174	1473.15	1.1	FI4
4	26.062249	2606.224906	1573.15	1.5	FI5

9.2   Comparing two EOS

DiadFit makes it very simple to compare calculations using the Sterner and Pitzer [1994] and Span and Wagner [1996] equation of states. Using linearly spaced vectors in Numpy, it is possible to perform thousands of calculations at different pressures, temperatures and densities. In Fig. 7, we perform calculations of pressure between 34 and 2000 °C for 11 discrete densities between 0.1 and 1.1 g/cm^3 (worked example given at ReadTheDocs). These calculations would have been extremely tedious in existing tools, but can be performed in several lines of code in DiadFit (and in seconds of computational time). This figure demonstrates that the EOS are extremely similar at the temperatures of basaltic magmas on Earth (<2% discrepancies).
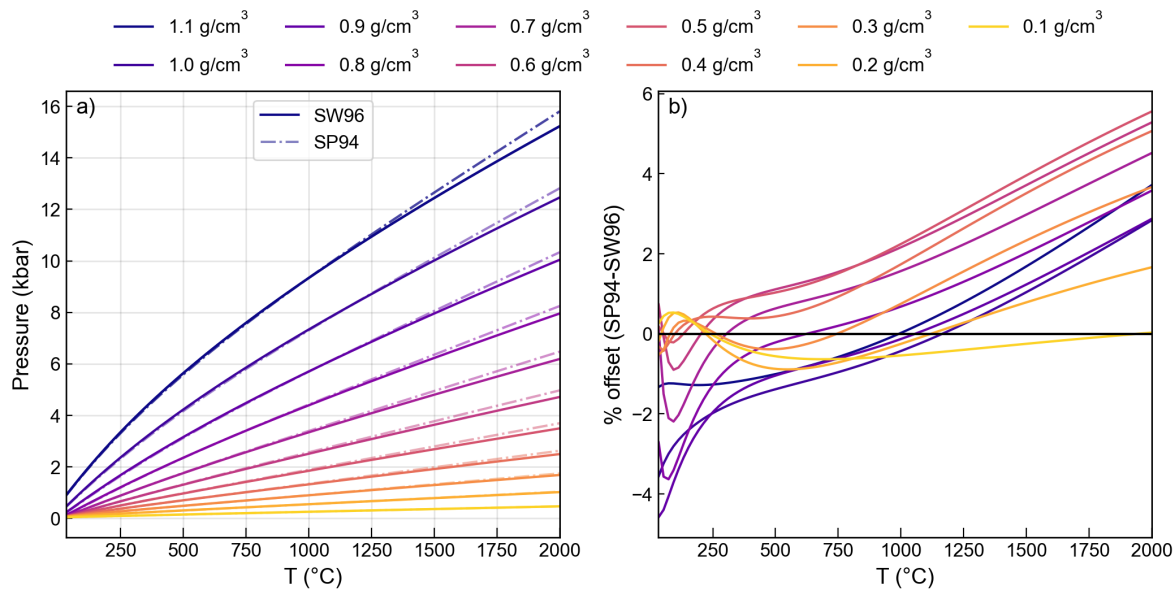
Figure 7: Comparison of the CO_2 EOS of Sterner and Pitzer [1994] and Span and Wagner [1996]. The y axis on b) shows the SP94-SW96 divided by the average of these two pressures.

9.3 Converting Pressures into depths

Building on functionality in Thermobar (Wieser et al. [2022]), DiadFit can convert entrapment pressures to depths using various options (Fig. 1h):

- A fixed crustal density (e.g., ρ=2700 kg/m^3)

- A 2-step crustal density profile (e.g., ρ=2700 kg/m^3 at <10 km, ρ=3300 kg/m^3 at >10 km)

- A 3-step crustal density profile

- Pressure-depth models of:

  1. Rasmussen et al. [2022] (`'rasmussen'`)
  2. the profile of Hill and Zuccal [1987] parameterized by Putirka [2017] (`'hill_zucca'`)
  3. the profile of Mavko and Thompson [1983] and DeBari and Greene [2011] parameterized by Putirka [2017] (`'mavko_debari'`)
  4. profile of Ryan [1988] parameterized by Lerner et al. [2021] (`'ryan_lerner'`).

We endeavor to add more profiles relevant to different tectonic settings as they become available.

Pressures should be converted into depth using the function `convert_pressure_to_depth`. For example, to calculate depths using the density profile of Lerner et al. [2021] for the pressures calculated above:

```
D_RL=pf.convert_pressure_to_depth(P_kbar=P_SW96['P_kbar']
model='ryan_lerner')
```

This returns a pandas Series of depths in km, which could be appended onto the dataframe produced above:

```
P_SW96['Depth_Ryan_Lerner']=D_RL
```

This function could be used to investigate a number of different pressure-depth conversions, appending each calculated depth onto a single dataframe for easy comparison.

9.4 Converting homogenization temperatures to CO_2 densities

The function `calculate_CO2_density_homog_T` calculates the density of CO_2 for a given homogenization temperature from microthermometry. Specifically, the homogenization temperature is the temperature at which a CO_2-rich fluid homogenises (e.g. a mix of liquid-vapour transitioning to a single homogenous phase). This observed temperature of homogenization is used to calculate a pressure based on the position of the L-V phase boundary. For a known pressure and temperature from the phase diagram, the CO_2 density can be calculated using an EOS for CO_2 (see Hansteen [1991], Kobayashi et al. [2012]).

We were only able to obtain the location of the L-V curve from Span and Wagner [1996]. For example, lets use this function to calculate the CO_2 density of a fluid inclusion which homogenized at –18 ° to a liquid phase:

```
CalcDens=pf.calculate_CO2_density_homog_T(
T_h_C=23, homog_to='L')
```

This returns a DataFrame showing the bulk density, the density of the co-existing liquid and vapour at this point on the phase diagram, and the user-inputted values.

	Bulk_gcm3	Liq_gcm3	Gas_gcm3	T_h_C	homog_to
0	1.022329	1.022329	0.055156	-18	L

Alternatively, an entire excel sheet of homogenization temperatures and phases can be loaded as a DataFrame. There is also an optional input of entering a sample name for each row (so it is returned in the outputted DataFrame):

```
pf.calculate_CO2_density_homog_T(
T_h_C=df['T_c_Homog'], SampleID=df['Sample'],
homog_to=df['homog_to'])
```

	Bulk_gcm3	Liq_gcm3	Gas_gcm3	T_h_C	homog_to	Sample_ID
0	0.593263	0.593263	0.345003	30	L	FI1
1	0.710471	0.710471	0.242710	25	L	FI2
2	0.773392	0.773392	0.194204	20	L	FI3
3	0.160735	0.821187	0.160735	15	V	FI4
4	0.861096	0.861096	0.135157	10	L	FI5

Uncertainties in homogenization temperature can be propagated to determine errors in density using Monte-Carlo techniques (see example on ReadTheDocs).

9.5 Propagating uncertainty using Monte Carlo techniques

DiadFit can be used to propagate uncertainty in input parameters, including uncertainty in CO_2 density resulting from uncertainty in homogenization temperature or Raman analyses, uncertainty in entrapment temperatures, and uncertainty in the method used to convert pressure into depth.

The function `propagate_FI_uncertainty` allows users to specify uncertainty in CO_2 density, temperature, and crustal density. For each input fluid inclusion, the function generates N duplicates of each input variable following the specified error distribution. Pressure (and depths) are then calculated for each of these N duplicates, which these are averaged to obtain the mean, median and standard deviation for each sample. Errors for each variable can be absolute (e.g., ±50 K for temperature) or percentage errors (e.g., ±5%), and error distributions can be normal or uniform. The function outputs a dataframe of all duplicates for all samples (e.g., if N=1000 duplicates and N=10 FIs, the dataframe has 10,000 rows), as well as a dataframe containing the average for each FI (e.g., mean pressure, standard deviation of pressure, mean depth, standard deviation of depth). This allows users to make figures of pressure or depths vs. parameters such as host Fo content, with error bars showing uncertainties in

depth for each FI. It also outputs a figure for one sample selected by the user to show the distribution of input and output parameters (Step 3, Fig. 8).

Figure 8: Schematic showing the workflow used to propagate uncertainty in CO_2 density, Temperature, and crustal density into error distributions in pressure and depth for each FI.

10 Quantifying peak asymmetry to identify co-existing liquid and gaseous CO_2

At room temperature (18-22 °C), CO_2 fluid with a density between ~0.18–0.21 and 0.75–0.79 g/cm^3 will consist of an inner shell of CO_2 vapour, and an outer shell of CO_2 liquid (Span and Wagner [1996]). For example, using the calculate_CO2_homog_T function, we can calculate that at 20 °C, the gaseous phase will have a density of 0.194 g/cm^3, and the liquid will have a density of 0.773 g/cm^3. De-Vitre et al. [2023] show that Raman measurements performed in these inclusions with two coexisting phases at room temperature and commonly-used laser powers don't always show two distinct peaks for the gaseous and liquid CO_2 phase, but often show a single skewed peak, with contributions from both phases. Quantifying peak asymmetry can help to identify spectra where both liquid and vapour were present.

To assess asymmetry in each spectra, an Nth degree polynomial is fitted between specified baseline positions (and this background is then subtracted). A cubic-spline is fitted between the baseline positions, and the x and y coordinate of the highest peak is identified. The position on each shoulder of the peak with an intensity equal to a certain fraction of the peak height is identified. In Fig. 9, this cut off parameter int_cut_off is set at 0.3. The ratio of the x-distance between the peak center and these shoulder points (green and grey lines in Fig. 9) defines the peak asymmetry. After tweaking these parameters for one spectra, the function loop_diad_skewness can be used to loop through all files in a specific folder, and stitch the results into a dataframe. Although critical parameters will have to be identified for each instrument, density estimates from spectra which show high asymmetry are unreliable, and should be recollected above the critical temperature of CO_2 (where liquid and vapour will have homogenized to a single supercritical phase, DeVitre et al. [2023]).

11 H_2O fitting

Raman spectroscopy can be used to quantify H_2O within silicate glasses (Di Genova et al. [2017]; Schiavi et al. [2018]). There are a number of different methods, with some using the height or intensity of the water Raman band (~3000-3800 cm^{-1}), and others using the ratio of the area under the water region divided by the area under the alumino-silicate band at ~200–1250 cm^{-1}. The exact relationship between this area ratio and the H_2O depends on instrument hardware and the glass major element composition, so standards with known H_2O contents must be used for calibration (Schiavi et al. [2018]). The sil-
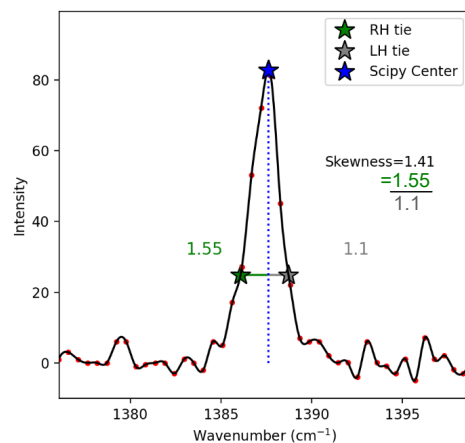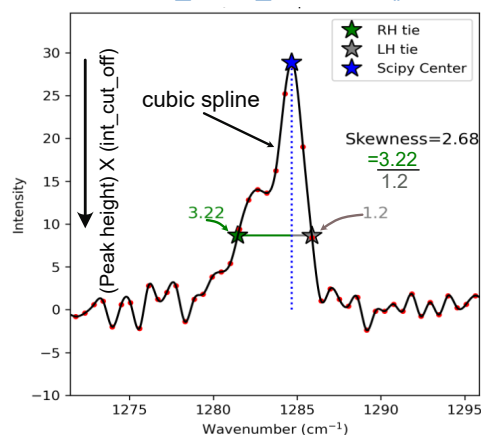
Figure 9: Schematic showing how DiadFit can be used to assess diad assymetry.

icate glass region consists of two bands, the low frequency/low wavenumber (LF or LW) band centered on ~550 cm^{-1} in Fig. 10, a medium frequency/wavenumber (MF, MW) band centered at ~550 cm^{-1}, and a high frequency/wavenumber (HF, HW) band at ~1000 cm^{-1}.

When fitting specta acquired on hydrous glasses in DiadFit, the first step is to select the files of interest. As for diads and Ne lines, we store default peak fit parameters in dataclasses. We have dataclasses for the four suggested background positions of Schiavi et al. [2018], e.g., `sil_bck_pos_Schiavi_basalt`, `sil_bck_pos_Schiavi_andesite`. Users can then tweak these background positions for their specific samples if they wish (e.g. for a basaltic andesite). These dataclasses are also used store the option for baseline fitting. By default, a polynomial of degree 3 is used. For example, the lower background position can be easily changed for basalt from the default of 300–340 to 320-350 cm^{-1}:

```
pf.sil_bck_pos_Schiavi_basalt(
lower_range_sil=[320, 350])
```

After subtracting away the background, an Nth degree polynomial is fitted to the silicate and water regions, and the area under each curve is calculated using the Simpson and the trapezoid method (Tallarida and Murray [1987]) implemented in SciPy and NumPy respectively. The function returns these areas, along with the ratio of the silicate to water areas for each area method (as well as other useful parameters such as the positions of choosen baselines, degrees of polynomials etc. for future reference).

Schiavi et al. [2018] aim to produce a global calibration, with less dependence on glass composition. They note that the baseline of the silicate region is highly dependent on glass composition and redox state, and suggest fitting a default cubic baseline through predefined baseline positions for 4 melt compositions (basalt, basanite, andesite, rhyolite). They find that the ratio of the total silicate area (LW+HW±MW) to H$_2$O area is reasonably independent of melt composition.

González-García et al. [2021] note that the presence of nanolites can complicate total silicate area methods, because they produce a peak at 670-690 cm^{-1} which can overlap with the LW silicate region used in the 'total area method' of Schiavi et al. [2018]. They propose a new protocol using only the HW area to characterize the silicate portion, rather than the the overall silicate region as in Schiavi et al. [2020]. DiadFit quantifies the HF, LF and -LW areas and the overall silicate area, to allow maximum flexibility (Fig. 10).

11.1 H$_2$O fitting within melt inclusions

A common problem when quantifying the amount of CO$_2$ within vapour bubbles comes from the presence of solid carbonate phases, which sequester carbon. The carbon held within these bubbles isn't accounted for using traditional Raman techniques Moore et al. [2015]. Devitre [2022] developed a technique where melt inclusions with carbonate-bearing vapour bubbles are heated to their liquidus temperature using a Linkam TS1400XY stage. The main concern regarding any heating method is that it causes diffusive loss of H$_2$O from melt inclusions (Gaetani et al. [2012]; Chen et al. [2011]).

Spectra acquired from melt inclusions which are not exposed is more complicated than quantification of exposed glass, because the acquired signal is a mix of the glass signal and signal from the olivine host. Before fitting the LW-HW silicate fits, the contribution from the host mineral must be subtracted to obtain an 'unmixed spectra', allowing reliable estimation of the silicate area. Here, we describe the method used for olivine-hosted melt inclusions, although it could be easily adapted for other phases. To reliably unmix the spectra, it is best to acquire a spectra in the melt inclusion at the depth where the H$_2$O peak is the strongest, and a spectra of the olivine next to the melt inclusions. DiadFit extracts the region of these two spectra between 800-900 cm^{-1} containing the strong olivine doublet. A cubic spline is fitted to both spectra to smooth out noise. SciPy is used to find the positions of the two strong peaks in the olivine spectra, and the trough position between these peaks. DiadFit then creates N spectra, where the olivine spectra is subtracted from the mixed spectra. For each of these mixed spectra, a linear regression is fit between the two points with the wavenumbers of the identified olivine peaks. The vertical (y) distance is then calculated between this linear regression and the y value at the x-cordinate of the trough (see Step 4, 11). When too little signal from the olivine has been subtracted from the mixed spectra, the trough position will be lower than the linear regression (e.g., Dist=-400 in sketch 1 on Fig. 11, and when too much olivine has been subtracted, the peaks will invert, and the distance will be a positive number. When exactly the right amount of olivine has been subtracted, there will be no clear peaks or troughs, so the distance will be zero. The function fits a curve to this calculated distance vs. the mixing proportion, to determine the best-fit mixing proportion where the distance is zero. The resulting, "unmixed" spectra is taken as the spectra from the melt inclusion itself. Then, the workflow discussed above can be applied to quantify the relative silicate and H$_2$O area.

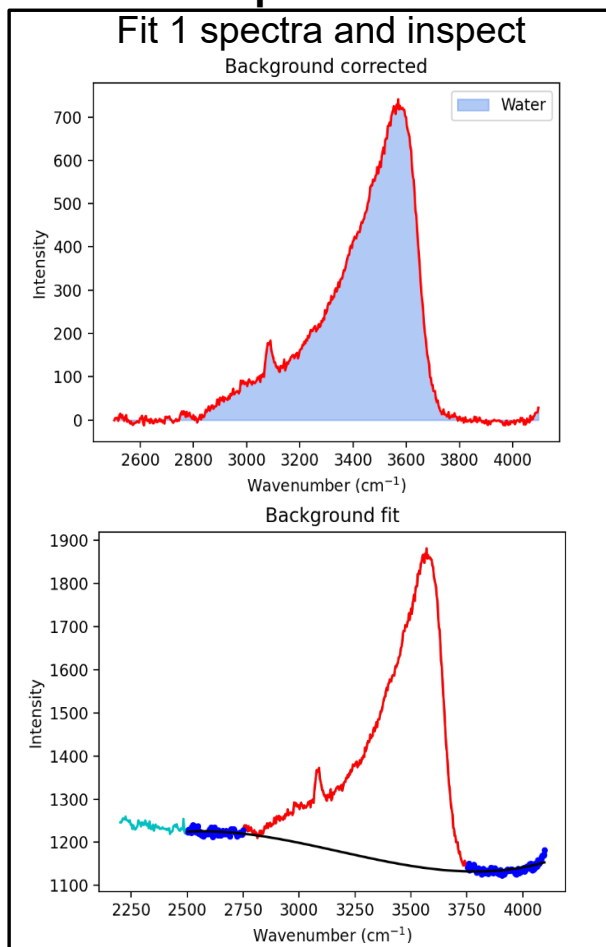Figure 10: Schematic showing how DiadFit can be used quantify the relative areas of silicate and H_2O peaks in Raman spectra collected from silicate glasses.

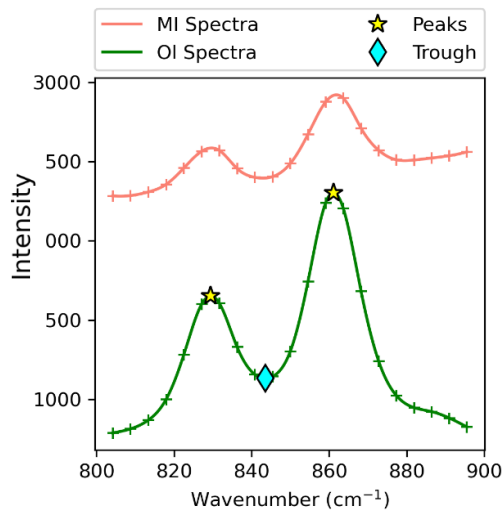# H₂O fitting in olivine-hosted melt inclusions (MIs)

Step 1

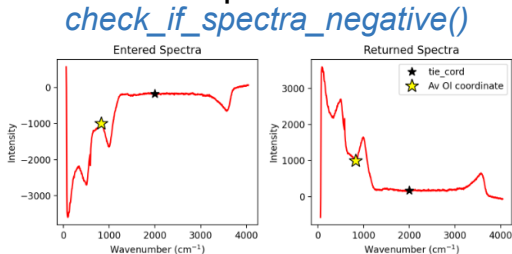Get filenames of spectra from MIs and neighbouring Ol crystals
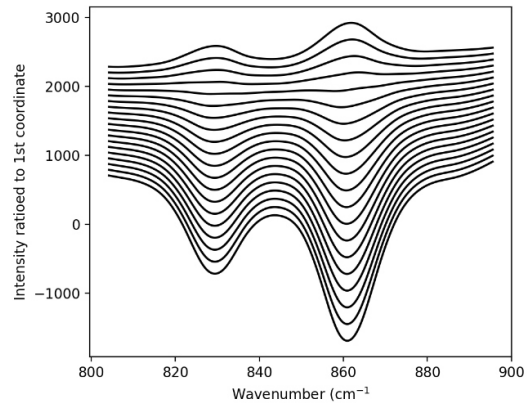
get_files()

Step 2

Find common parts of file name (e.g., xstal, MI name) to pair up MI+Ol files. Select 1 pair.

extract_xstal_MI_name()

filename_x	crystal_name	MI_name	filename_y
02 CC14_MI2_H2O_96mw.txt	CC14	MI2	03 CC14_MI2_Ol_96mw.txt
05 CC13_MI4_H2O.txt	CC13	MI4	06 CC13_MI4_Ol.txt

Step 3

Extra region around ~800-900 cm⁻¹ for both spectra. Fit a smoothed cubic spline + ID peaks and troughs

get_spectra(),
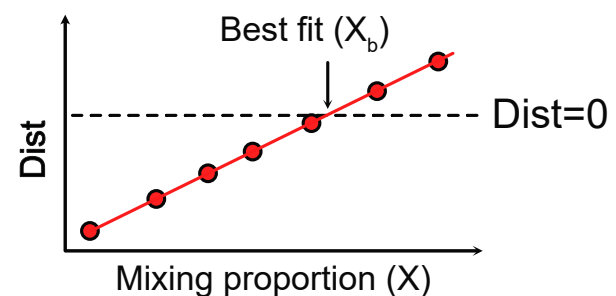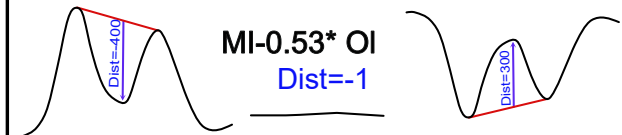*smooth_and_trim_around_olivine()*

Step 4

Subtract varying proportions of Ol from the MI spectra.

make_evaluate_mixed_spectra()

Best match when y distance between 2 peaks and trough is as small as possible in unmixed spectra

Step 5

Check if unmixed spectra inverted (using 2 tiepoints). Flip if so

check_if_spectra_negative()

Step 6+ = See 'H₂O fitting in silicate glasses'

Figure 11: Schematic showing how DiadFit can be used to unmix the contribution of olivine and glass from spectra taken on unexposed melt inclusions. The code could be easily adapted for other silicate phases. There is an option to loop if glass compositions are sufficiently similar. Alternatively, each file can be stepped through manually to tweak positions, and the code saves the output for each file to a .csv, and these are then stitched together after all files are fitted.

12   Future Work

The open-source nature of DiadFit means that users can customize functions and build their own (either on a local fork, or using a pull request on GitHub). Additionally, we anticipate that we will continue to add workflows as new applications of Raman spectroscopy appear in volcanology. To reflect the evolving nature of this tool, when citing DiadFit, users should make sure they specify the version they used, obtained using:

```
pf.__version__
```

Care should also be taken to cite the root packages used by DiadFit. E.g., if converting CO$_2$ densities to pressures using the functions here, we recomend wording similar to this: "CO$_2$ densities were converted into pressures using DiadFit (Wieser and DeVitre, 2023, v.1.0), using the Equation of State of Span and Wagner [1996] implemented in CoolProp (Bell et al. [2014]).

13   Conclusions

DiadFit will greatly reduce the time required to fit Raman spectral data for volcanological applications, as well as increasing reproducibility between studies. Less time peak fitting = more time for science!

Author contributions

PW conceived the project, and wrote the majority of the code, with discussions with CD of how best to implement various procedures. CD wrote the cosmic ray removal code, and performed extensive testing and tweaking of existing functions.

Data availability

All files are available on GitHub https://github.com/PennyWieser/DiadFit. Documentation is available at ReadTheDocs (bit.ly/DiadFitRTD), and YouTube videos explaining various aspects of the tool are available on Penny Wieser's YouTube channel bit.ly/DiadFitYouTube.

Presses universitaires de Strasbourg

References

Allison, C. M., Roggensack, K., and Clarke, A. B. (2021). Highly explosive basaltic eruptions driven by co2 exsolution. *Nature communications*, 12(1):1–10.

Bakker, R. J. (2021). The perfection of raman spectroscopic gas densimeters. *Journal of Raman Spectroscopy*, 52(11):1923–1948.

Bell, I. H., Wronski, J., Quoilin, S., and Lemort, V. (2014). Pure and pseudo-pure fluid thermophysical property evaluation and the open-source thermophysical property library coolprop. *Industrial & engineering chemistry research*, 53(6):2498–2508.

Burke, E. A. (2001). Raman microspectrometry of fluid inclusions. *Lithos*, 55(1-4):139–158.

Chen, Y., Provost, A., Schiano, P., and Cluzel, N. (2011). The rate of water loss from olivine-hosted melt inclusions. *Contributions to Mineralogy and Petrology*, 162:625–636.

Dayton, K., Gazel, E., Wieser, P., Troll, V. R., Carracedo, J. C., La Madrid, H., Roman, D. C., Ward, J., Aulinas, M., Geiger, H., et al. (2023). Deep magma storage during the 2021 la palma eruption. *Science Advances*, 9(6):eade7641.

DeBari, S. M. and Greene, A. R. (2011). Vertical stratification of composition, density, and inferred magmatic processes in exposed arc crustal sections. In *Arc-continent collision*, pages 121–144. Springer.

DeVitre, C., Dayton, K., Gazel, E., Pamukcu, A., Gaetani, G., and Wieser, P. (2023). Laser heating effect on raman analysis of co2 co-existing as liquid and vapor in olivine-hosted melt inclusion bubbles. *Volcanica*.

DeVitre, C. L., Allison, C. M., and Gazel, E. (2021). A high-precision co2 densimeter for raman spectroscopy using a fluid density calibration apparatus. *Chemical Geology*, 584:120522.

Devitre, C. L. J. (2022). *Magmatic Drivers of Explosive Volcanism: Insight from Magma Mixing, Melt Inclusions and Raman Spectroscopy*. PhD thesis. Copyright - Database copyright ProQuest LLC; ProQuest does not claim copyright in the individual underlying works; Last updated - 2023-03-10; SubjectsTermNotLitGenreText - Cape Verde Islands; Costa Rica.

Di Genova, D., Sicola, S., Romano, C., Vona, A., Fanara, S., and Spina, L. (2017). Effect of iron and nanolites on raman spectra of volcanic glasses: A reassessment of existing strategies to estimate the water content. *Chemical Geology*, 475:76–86.

Fermi, E. (1931). Über den ramaneffekt des kohlendioxyds. *Zeitschrift für Physik*, 71:250–259.

Frezzotti, M. L., Tecce, F., and Casagli, A. (2012). Raman spectroscopy for fluid inclusion analysis. *Journal of Geochemical Exploration*, 112:1–20.

Fukura, S., Mizukami, T., Odake, S., and Kagi, H. (2006). Factors determining the stability, resolution, and precision of a conventional raman spectrometer. *Applied Spectroscopy*, 60(8):946–950.

Gaetani, G. A., O'Leary, J. A., Shimizu, N., Bucholz, C. E., and Newville, M. (2012). Rapid reequilibration of h_2o and oxygen fugacity in olivine-hosted melt inclusions. *Geology*, 40(10):915–918.

Giordano, D., Russell, J. K., González-García, D., Bersani, D., Dingwell, D. B., and Del Negro, C. (2020). Raman spectroscopy from laboratory and proximal to remote sensing: a tool for the volcanological sciences. *Remote Sensing*, 12(5):805.

González-García, D., Giordano, D., Allabar, A., Andrade, F., Polo, L., Janasi, V. d. A., Lucchetti, A., Hess, K.-U., De Campos, C., and Dingwell, D. (2021). Retrieving dissolved h2o content from micro-raman spectroscopy on nanolitized silicic glasses: application to volcanic products of the paraná magmatic province, brazil. *Chemical Geology*, 567:120058.

González-García, D., Giordano, D., Russell, J. K., and Dingwell, D. B. (2020). A raman spectroscopic tool to estimate chemical composition of natural volcanic glasses. *Chemical Geology*, 556:119819.

Hansteen, T. H. (1991). Multi-stage evolution of the picritic maelifell rocks, sw iceland: constraints from mineralogy and inclusions of glass and fluid in olivine. *Contributions to Mineralogy and Petrology*, 109(2):225–239.

Hansteen, T. H. and Klugel, A. (2008). Fluid inclusion thermobarometry as a tracer for magmatic processes. *Reviews in Mineralogy and Geochemistry*, 69(1):143–177.

Harris, C. R., Millman, K. J., van der Walt, S. J., Gommers, R., Virtanen, P., Cournapeau, D., Wieser, E., Taylor, J., Berg, S., Smith, N. J., et al. (2020). Array programming with numpy. *Nature*, 585(7825):357–362.

Hartley, M. E., Maclennan, J., Edmonds, M., and Thordarson, T. (2014). Reconstructing the deep co2 degassing behaviour of large basaltic fissure eruptions. *Earth and Planetary Science Letters*, 393:120–131.

Hill, D. P. and Zuccal, J. J. (1987). Geophysical constraints on the structure of. *US Geological Survey Professional Paper*, 2(1350):903.

Hunter, J. D. (2007). Matplotlib: A 2d graphics environment. *Computing in Science & Engineering*, 9(3):90–95.

Kobayashi, T., Yamamoto, J., Hirajima, T., Ishibashi, H., Hirano, N., Lai, Y., Prikhod'Ko, V. S., and Arai, S. (2012). Conformity and precision of co2 densimetry in co2 inclusions: Microthermometry versus raman microspectroscopic densimetry. *Journal of Raman Spectroscopy*, 43(8):1126–1133.

Lamadrid, H., Moore, L., Moncada, D., Rimstidt, J., Burruss, R., and Bodnar, R. (2017). Reassessment of the raman co2 densimeter. *Chemical Geology*, 450:210–222.

Lerner, A. H., Wallace, P. J., Shea, T., Mourey, A. J., Kelly, P. J., Nadeau, P. A., Elias, T., Kern, C., Clor, L. E., Gansecki, C., et al. (2021). The petrologic and degassing behavior of sulfur and other magmatic volatiles from the 2018 eruption of kīlauea, hawaii: melt concentrations, magma storage depths, and magma recycling. *Bulletin of Volcanology*, 83(6):1–32.

Lin, F., Bodnar, R., and Becker, S. (2007). Experimental determination of the raman ch4 symmetric stretching ($v1$) band position from 1–650 bar and 0.3–22 c: Application to fluid inclusion studies. *Geochimica et Cosmochimica Acta*, 71(15):3746–3756.

Mavko, B. B. and Thompson, G. A. (1983). Crustal and upper mantle structure of the northern and central sierra nevada. *Journal of Geophysical Research: Solid Earth*, 88(B7):5874–5892.

Moore, L. R., Gazel, E., Tuohy, R., Lloyd, A. S., Esposito, R., Steele-MacInnis, M., Hauri, E. H., Wallace, P. J., Plank, T., and Bodnar, R. J. (2015). Bubbles matter: An assessment of the contribution of vapor bubbles to melt inclusion volatile budgets. *American Mineralogist*, 100(4):806–823.

Morizet, Y., Brooker, R. A., Iacono-Marziano, G., and Kjarsgaard, B. A. (2013). Quantification of dissolved co2 in silicate glasses using micro-raman spectroscopy. *American Mineralogist*, 98(10):1788–1802.

Newville, M., Stensitzki, T., Allen, D. B., Rawlik, M., Ingargiola, A., and Nelson, A. (2016). Lmfit: Non-linear least-square minimization and curve-fitting for python. *Astrophysics Source Code Library*, pages ascl–1606.

pandas development team, T. (2020). pandas-dev/pandas: Pandas.

Putirka, K. D. (2017). Down the crater: where magmas are stored and why they erupt. *Elements*, 13(1):11–16.

Rasmussen, D. J., Plank, T. A., Roman, D. C., and Zimmer, M. M. (2022). Magmatic water content controls the pre-eruptive depth of arc magmas. *Science*, 375(6585):1169–1172.

Roedder, E. (2018). Reviews in mineralogy. In *Fluid inclusions*, pages II–II. De Gruyter.

Rosso, K. and Bodnar, R. (1995). Microthermometric and raman spectroscopic detection limits of co$_2$ in fluid inclusions and the raman spectroscopic characterization of c02. *Geochimica et Cosmochimica Acta*, 59(19):3961–3975.

Ryan, M. P. (1988). The mechanics and three-dimensional internal structure of active magmatic systems: Kilauea volcano, hawaii. *Journal of Geophysical Research: Solid Earth*, 93(B5):4213–4248.

Schiavi, F., Bolfan-Casanova, N., Buso, R., Laumonier, M., Laporte, D., Medjoubi, K., Venugopal, S., Gómez-Ulla, A., Cluzel, N., and Hardiagon, M. (2020). Quantifying magmatic volatiles by raman microtomography of glass inclusion-hosted bubbles. *Geochemical Perspectives Letters*, 16:17–24.

Schiavi, F., Bolfan-Casanova, N., Withers, A. C., Médard, E., Laumonier, M., Laporte, D., Flaherty, T., and Gómez-Ulla, A. (2018). Water quantification in silicate glasses by raman spectroscopy: Correcting for the effects of confocality, density and ferric iron. *Chemical Geology*, 483:312–331.

Span, R. and Wagner, W. (1996). A new equation of state for carbon dioxide covering the fluid region from the triple-point temperature to 1100 k at pressures up to 800 mpa. *Journal of physical and chemical reference data*, 25(6):1509–1596.

Steele-Macinnis, M., Esposito, R., and Bodnar, R. J. (2011). Thermodynamic model for the effect of post-entrapment crystallization on the h2o–co2 systematics of vapor-saturated, silicate melt inclusions. *Journal of Petrology*, 52(12):2461–2482.

Sterner, S. M. and Pitzer, K. S. (1994). An equation of state for carbon dioxide valid from zero to extreme pressures. *Contributions to Mineralogy and Petrology*, 117(4):362–374.

Tallarida, R. J. and Murray, R. B. (1987). Area under a curve: trapezoidal and simpson's rules. In *Manual of Pharmacologic Calculations*, pages 77–81. Springer.

Virtanen, P., Gommers, R., Oliphant, T. E., Haberland, M., Reddy, T., Cournapeau, D., Burovski, E., Peterson, P., Weckesser, W., Bright, J., van der Walt, S. J., Brett, M., Wilson, J., Millman, K. J., Mayorov, N., Nelson, A. R. J., Jones, E., Kern, R., Larson, E., Carey, C. J., Polat, İ., Feng, Y., Moore, E. W., VanderPlas, J., Laxalde, D., Perktold, J., Cimrman, R., Henriksen, I., Quintero, E. A., Harris, C. R., Archibald, A. M., Ribeiro, A. H., Pedregosa, F., van Mulbregt, P., and SciPy 1.0 Contributors (2020). SciPy 1.0: Fundamental Algorithms for Scientific Computing in Python. *Nature Methods*, 17:261–272.

Wang, W. and Lu, W. (2022). High-precision carbon isotopic composition estimation for individual co2 fluid inclusions through raman spectroscopy. *Geoscience Frontiers*, page 101528.

Wang, X., Chou, I.-M., Hu, W., Burruss, R. C., Sun, Q., and Song, Y. (2011). Raman spectroscopic measurements of co2 density: Experimental calibration with high-pressure optical cell (hpoc) and fused silica capillary capsule (fscc) with application to fluid inclusion observations. *Geochimica et Cosmochimica Acta*, 75(14):4080–4093.

Wieser, P., Petrelli, M., Lubbers, J., Wieser, E., Ozaydin, S., Kent, A., and Till, C. (2022). Thermobar: an open-source python3 tool for thermobarometry and hygrometry. *Volcanica*, 5(2):349–384.

Wieser, P. E., Lamadrid, H., Maclennan, J., Edmonds, M., Matthews, S., Iacovino, K., Jenner, F. E., Gansecki, C., Trusdell, F., Lee, R. L., et al. (2021). Reconstructing magma storage depths for the 2018 kılauean eruption from melt inclusion co2 contents: the importance of vapor bubbles. *Geochemistry, Geophysics, Geosystems*, 22(2):e2020GC009364.

Wojdyr, M. (2010). Fityk: a general-purpose peak fitting program. *Journal of Applied Crystallography*, 43(5-1):1126–1128.

Yuan, X. and Mayanovic, R. A. (2017). An empirical study on raman peak fitting and its application to raman quantitative research. *Applied spectroscopy*, 71(10):2325–2338.